Original research article

The study of mechanical and statistical properties of nitrogen ion-implanted Tantalum bulk

A.H. Ramezani [a],*, S. Hoseinzadeh [b],*, Zh. Ebrahiminejad [a], M.R. Hantehzadeh [c], M. Shafiee [d]

[a] *Department of Physics, West Tehran Branch, Islamic Azad University, Tehran, Iran*
[b] *Department of Mechanical and Aeronautical Engineering, University of Pretoria, Pretoria, South Africa*
[c] *Plasma Physics Research Centre, Science and Research Branch, Islamic Azad University, Tehran, Iran*
[d] *School of Engineering and Digital Arts, University of Kent, Canterbury, CT2 7NT, United Kingdom*

ARTICLE INFO

ABSTRACT

In the present study, structural and mechanical properties of Tantalum samples which affected by nitrogen ion implantation have been investigated. The monofractal analysis of the samples has been carried out. These samples have been implanted with ions at different doses of 5×10^{17} and 7×10^{17} at energy 30 keV. For characterizing the samples, atomic force microscopy (AFM), EDX images analysis, and corrosion measurements, have been used. By varying the ion energy, the statistical characteristics will vary. In order to analyse the morphology of produced rough samples, the correlation function of samples have been studied and their correlation length is evaluated. Based on the statistical concept the power spectral density the height distribution, and the higher-order moments (skewness and kurtosis) of the surface height have been measured. These charactristics are the important criterions for the the monofractal evaluation. Our numerical calculations based on experimental data show the deviation from gaussian distribution. Also, the fractal dimension of the films has been calculated based on rougness exponent results. Indeed, irradiating the surfaces with energetic ions results in producing the self-affine fractal surfaces. This process via an erosion process affects the statistical characteristics which have been calculated for different samples. Because of variation in the morphology of rough samples, the corrosion of samples shows a non-uniform behavior.

1. Introduction

For many years, the tantalum has been used in various experimental projects because of its low density, high corrosion resistance, and excellent biocompatibility [1–3]. The sputtering, ion implantation and ion coating are the different approaches for improving the tantalum surface [4]. To improve the surface of tantalum, Carbon, Nitrogen and Oxygen have been utilized. The Nitrogen implantation has been commonly used because it allows the growth of the film keeping the substrate at low or moderate temperatures [5–7]. The produced Titanium nitride surfaces are suitable to characterize the ultrathin films with a surface sensitive technique. Some parameters such as ion energy, temperature, density of current and irradiation time play the key role in surface characteristics through ion bombardment. Indeed, the growth conditions have the impressive effect on mechanical, electrical, and optical properties of produced
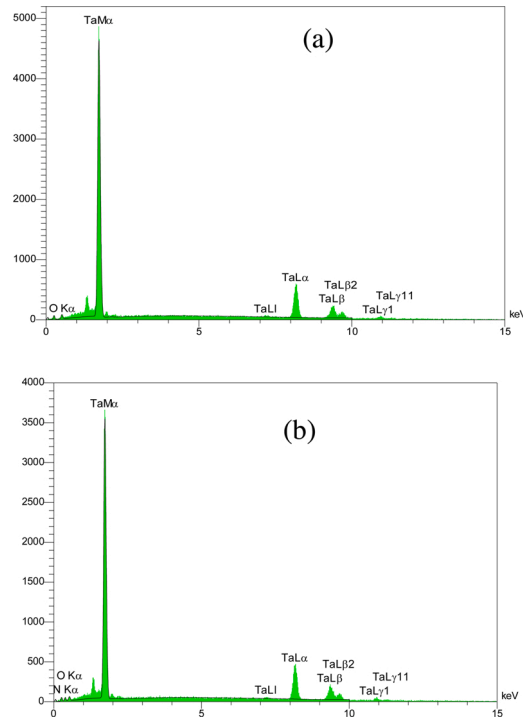

Fig. 1. EDX analysis of (a) unimplanted sample, and (b) implanted (with dose 5×10^{17} ion/cm^2) samples.

samples [8]. There are various methods to generate the rough surfaces [10] which are generally expected to have self-affine fractal behaviors [11,12]. The ion implantation is a process which leads to production of thin films with stochastic and nonequilibrium characteristics. Therefore, the scaling theories have been used to investigate the morphology of produced surfaces [9,12]. As the energy of ion beams varies, the surface characteristics change. Indeed, the morphology of the surfaces is expected to be influenced by nitrogen ion implantation [13]. In some works improving the corrosion resistance of thin films by nitrogen ion implantation [14] and the fractal feature of thin films surfaces modified by low energy nitrogen ion [15] have been analyzed. There are several methods such as 'blanket' fractal analysis [16], 'skyscraper' fractal analysis [17], and the box counting method [18] for investigating the fractality behavior of the experimentally generated thin films [19–22].The aim of this work is investigation the effect of ion-implantation on mechanical and statistical properties of different samples which are unimplanted /implanted by different ion doses. In the present study, Tantalum nitride thin films were grown by fixed-energy nitrogen and different ion doses at room temperature. The roughness, corrosion resistance, microhardness testing, friction coefficient measurements, and wear mechanism have been evaluated by using the AFM and the Scanning electron microscope (SEM) analysis. Here, these samples morphology based on monofractal analysis have been investigated. The height fluctuations, power spectral density, skewness, kurtosis, correlation function, and correlation length of samples are the characteristics which have been calculated. Also, the roughness exponent and therefore the fractal dimension of different samples have been estimated.

The reminder of this paper is organized as follow. In Section 2, the materials and experimental details of samples preparation are explained. The statistical analysis and the measurements (surface and corrosion) results and discussions are described in Section 3. Finally, the Section 4 devotes to conclusion and remarks.

2. Preparation of samples

The sample which cut into 1 cm × 1 cm and 0.58 mm thickness is exposed to nitrogen ion implantation. The Nitrogen ions land on sample vertically and their energy and doses of (99.999 %) were 30 keV and 1×10^{17} to 9×10^{17} ions/cm^2 at ambient temperature. In present work, the microstructure of the samples before and after ion implantation is characterized by EDX images using STOE model STADI MP system using Cu kα radiation (wavelength = 1.5405 Å) with a tungsten filament at 40 kV, 40 mA and step size of 0.04. The implantation-induced modification of surface roughness is studied by employing an atomic force microscopy (AFM). The facility was an AFM (SPM Auto Probe CP, Park Scientific Instruments, USA) in contact mode with low stress. In the following the measurements are described in details.

The samples and the time of ion bombardment have been presented in Tale 1.

The I_{corr}, the temperature and E_{corr} have the fixed values 100 μA/cm^2, 100 K and 30KeV for all samples, respectively. Also, the temperature reached a maximum steady value of 100 ℃.

The EDX images of the two (un-implanted and implanted) samples have been presented in Fig. 1. Based on the results, the nitrogen
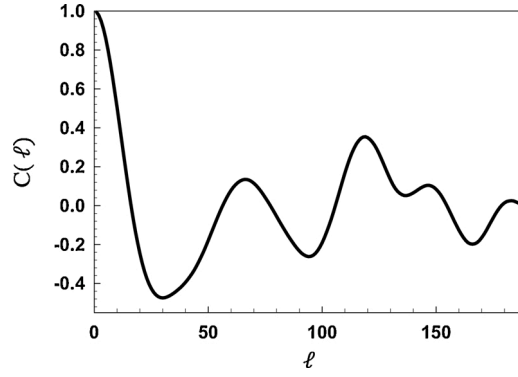
Fig. 2. The correlation function as a function of separation distance for unimplanted sample.
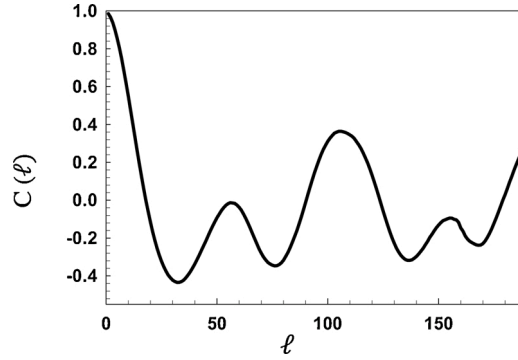

Fig. 3. The correlation function as a function of separation distance for sample 3.

ions can be observed in implanted sample (b).

3. Results and discussion

3.1. Statistical analysis

The random rough surfaces, mathematically described as h(i,j) is studied in terms of its deviation from a smooth surface. The root-mean-square (RMS) is defined as follow

$$\text{RMS} = \sqrt{\left\langle h(r)^2 \right\rangle}, \tag{1}$$

This parameter is most important for characterizing the rough surfaces. $h(r)$ represents the height at position r [9]. The RMS roughness of samples have been displayed in Table 2.

Generally, the AFM is a suitable technique to investigate the surface roughness and scaling parameters. Based on AFM analysis, the values of average roughness as a function of ion dose for various samples are presented in Table 3. As the ion dose increases; the surface morphology has a significant change and a notable growth in the surface roughness appear.

Ion bombardment can cause to surface diffusion mechanism which results in the roughness enhancement. Moreover, the roughness reduction may be because of higher sputtering rate through ion bombardment [12].

Description of the height variations could be obtained by the average surface roughness but it not included any information about the waviness. The root-mean-square is more sensitive to deviation from the smooth plane; however, it does not present the comprehensive explanation of the rough surfaces. In order to describe the rough surfaces, the correlation function, C(R), has been described. The manner of height variation along the surface is described with C(R); indeed it describes the correlation property of heights at two positions that are R point away along the surface. The normalized C(R), is defined as follow

$$C(\text{R}) = \frac{\langle h(r_1) h(r_2) \rangle}{(\text{RMS})^2}, \tag{2}$$

which, R is the separation distance between two points. The distance which the C(R) falls to $1/e$ of its maximum value named as the correlation length, λ [23,24]. As it can be seen in Figs. 2 and 3, the correlation functions of unimplanted and implanted samples with
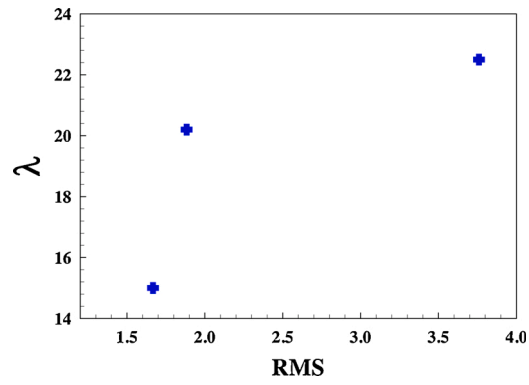
3

Fig. 4. The variation of correlation length and RMS for different samples.

Table 1
Ion implantation data.

Sample	Dose	Time
1	unimplanted	——————
2	5×10^{17}	700s
3	7×10^{17}	1120s

Table 2
The RMS height of un-implanted and implanted samples.

sample	1	2	3
RMS(Å)	1.667	1.883	3.760

Table 3
Variation of average roughness for different samples.

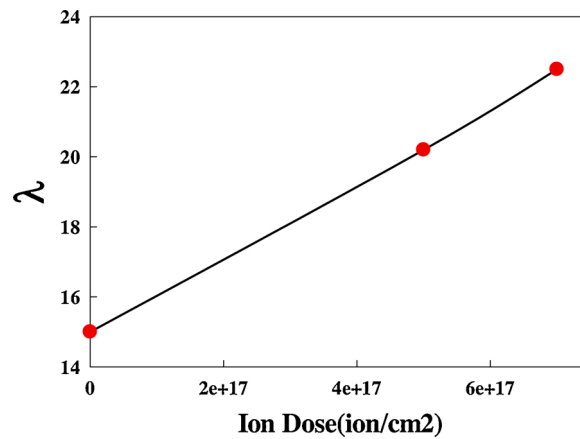| Dose (ion/cm^2)	Average Roughness(Å)
Unimplanred	1.269
5×10^{17}	1.399
7×10^{17}	2.894

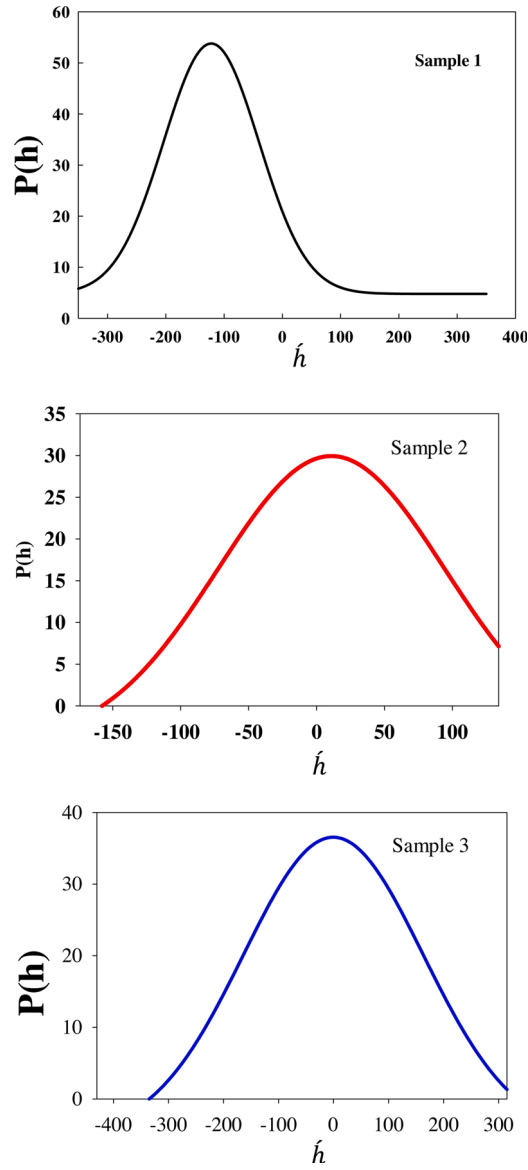**Fig. 5.** Correlation length versus Ion dose.

Fig. 6. The normalized height distribution for unimplanted and implanted samples.

respect to the separation distance R has the same behavior and it reduces by increasing the R value. Based on Eq (2), for points with large distance, C(R) comes to be zero. Through the surface growth, at first, the height of sites is not dependent on neighboring sites [9].

The variation of correlation length and RMS for different samples has been shown in Fig. 4 simultaneously.

With increasing the RMS (increasing ratio of $RMS/_\lambda$) the surface roughening increases [25,26]. Based on results of Fig. 4, the sample 2 is rougher rather than the other samples. This results are agreed the results of Table 1.

Fig. 5, shows the variation of correlation length as a function of Nitrogen dose. As it is seen in figure, the correlation length increases with increasing the ion dose.

In other words, as it is expected with increasing the ion doses, the rough implanted surfaces will be more correlated.

3.2. Surface height distribution

Through the monofractal analysis, the symmetric or asymmetric behavior of the surface height distribution and its deviation from the Gaussian have been investigated. The height distribution and the 3rd- and 4th-order moments (the two higher order moments) present the information about the surface morphology.

Skewness is the 3rd moment of height distribution which measures the symmetry distribution.

Table 4
The roughness exponent of all samples.

sample	1	2	3
Roughness exponent	0.803	0.695	0.77

Table 5
The fractal dimension of unimplanted and implanted samples.

sample	1	2	3
fractal dimension	1.197	1.305	1.23

$$skewness = \frac{\left\langle (h - \overline{h})^3 \right\rangle}{\left\langle \left(h - \overline{h} \right)^2 \right\rangle^{3/2}} , \tag{3}$$

skewness sign indicates that the data points are skewed to the left (negative sign) or to the right (positive sign) of the data average [27].

The kurtosis is the 4th-order moment of surface height and it equals to 3 for Gaussian distribution. It defined as [27]

$$kurtosis = \frac{\left\langle (h - \overline{h})^4 \right\rangle}{\left\langle \left(h - \overline{h} \right)^2 \right\rangle^2} , \tag{4}$$

R_{ku} determines the sharpness of the height distribution function. In other words it is a measure of the fatness (kurtosis<3) or the sharpness (kurtosis>3) peak of the probability.

The skewness is negative (skewness = −1.01) and positive (skewness = 1.001) for unimplanted and implanted samples, respectively. Also, the measure of kurtosis shows the deviation from the Gaussian distribution, (where kurtosis = 3). The results show the kurtosis is less than three for all samples. Indeed, the low valleys and more high peaks over the thin films exist. Therefore, the asymmetric tail and nonzero skewness are the reasons for deviation from Gaussian distribution [28,29]. The results measured for skewness and kurtosis of samples show the deviation of Gaussian distribution.

Moreover the higher order moments of height distribution, the power spectrum can measure and describe the spread of the heights above the mean surface and also the height variation along the surface. Mathematically it is the Fourier transform of correlation

$$P(k) = \frac{1}{2\pi} \int C(\ell) e^{ik.\ell} d\ell, \tag{5}$$

when the height of the points is measured with respect to mean height ($h^{'} = h - \overline{h}$).The normalized height distribution P(h) has been obtained In reference [29].

The distribution's deviation from the Gaussian one which confirms the results of skewness and kurtosis have been presented in Fig. 6.

3.3. Roughness exponent and Fractal dimension

For a rough surface, the width is defined as below

$$w(L,t) = \sqrt{\left\langle \left(h(i,t) - \overline{h}(t) \right)^2 \right\rangle}, \tag{6}$$

Which, $\overline{h}(t)$ is the average height at time t and h(i,t) is the surface height at site i and time t. The surfaces which saturated in enough long times, the roughness width (w) has a power law dependency on substrate size (L) as [9]

$$w_L = L^H, \tag{7}$$

where, the exponent *H* is the roughness exponent which also is called Hurst exponent [30–32]. This exponent is used to analysis the irregularity or smoothness of surfaces [25,26]. In Table 4, the roughness exponent of unimplanted and implanted samples have been presented.

These results confirm the results which have been obtained in Fig. 4. The sample 2 has the heights ratio of RMS$/_\lambda$ and also has the lowest roughness exponent. The lower amount of roughness exponent characterizes jagged or irregular surfaces at short length scales [25,26].

In a self-affine surface, a portion of surface statistically is identical to its entire if different magnifications are used [34–36]. With increasing the ion bombardment time, the surface width (W) increases, and the surface is named self-affine when the W increases with
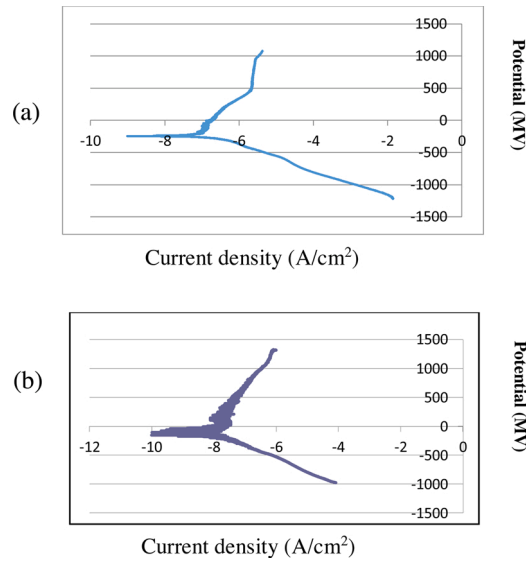
Fig. 7. Corrosion potential as a function of potential for un-implanted (a) and implanted (b) samples.

horizontal length. W has a power law dependency on the substrate size according to Eq. (7). The roughness exponent is in the range $0 \leq H \leq 1$ for self-affine surfaces [9].

The fractal dimension, D_f, which is a measure of the surface complexity is straightly related to roughness exponent. Among the different approaches of calculating the fractal dimension [9,28], one can obtain it as $D_f = 1 + 1 - H$. The $(1 + 1)$ is considered for profiles. The fractal dimensions of samples have been measured and presented in Table 5.

The monofractal analysis of different samples revealed that they have the fractal behavior.

3.4. Corrosion test results

Nitrogen ion implantation causes to corrosion potential enhancement which it increases and then decreases in the implanted samples [33]. The values of corrosion potential as a function of current density (A/cm^2) for implanted and un-implanted samples is showed in Fig. 7.

The corrosion rate decreases with increasing the nitrogen dose. On the other side, the samples have been more correlated with increasing the ion dose. Although these conditions seem more suitable with regarding the corrosion rates, but it can be mentioned that with regard to corrosion morphology and pit formation, corrosion occurrence conditions have stepped up. From the viewpoint of corrosion, local corrosions show less corrosion current density; but because this corrosion penetrates to piece depth, the occurred damages are more severe. As the ionized atoms' dose increases, the amount of nitrogen implanted in the layer increases and it decreases as the corrosion-resistive layers decreases. However, the implanted layer cannot resist the corrosion due to insufficiency of dose. Consequently, local corrosion and pit formation is observed on the surface of corroded sample. Varying the surface roughness and morphology of samples results in a non-uniform corrosion of samples. Through the ion implantation, a higher sputtering rate may occur, thus the roughness decreases at some doses. Indeed, through an etching process or surface diffusion can occur through entering nitrogen ions into the samples which can decrease the roughness.

4. Conclusion

The Effect of Nitrogen ion-implantation with different doses on mechanical and statistical properties of Tantalum bulk have been studied. The monofractal analysis show the fractal ehavior of different samples. The results of measurment the skewness and kurtosis show the deviation from Gaussian distribution which has been confirmed with plotting the normalized height distribution. Also, the roughness exponent and fractal dimension of different samples have been evaluated. The corrosion rate decreases with increasing the nitrogen dose. The corrosion potential enhancement is a consequence of nitrogen ion implantation. As the ion doses increases the correlation along the samples develops, thus the correlation length increases. The corrosion rate decreases with increasing the nitrogen dose. The non-uniform corrosion of samples appears because of variation the surface roughness and morphology of samples. It is appeared that in the ion dose 5×10^{17}(ion/cm^2), the sample is rougher than the others. The results show that the unimplanted and ion implanted surfaces generate the self-affine surfaces and they were in a well agreement with experimental results. This approach can be generalized for various ranges of grown thin films by different methods.

Declaration of Competing Interest

The authors reported no declarations of interest.

References

[1] R. Hübler, Surf. Coat. Technol. 116 (1999) 1111.
[2] S. Saritas, R.P.M. Procter, W.A. Grant, Mater. Sci. Eng. A 115 (1989) 307.
[3] F. Hellal, F. Atmani, B. Malki, H. Sedjal, M. Kerkar, F. Dalard, (2006) 371.
[4] I.N. Andijani, S. Ahmad, A.U. Malik, Desalination 129 (2000) 45.
[5] G.S. Chen, S.T. Chen, J. Appl. Phys. 87 (2000) 8473.
[6] J. Chuang, M. Chen, Thin Solid Films 322 (1998) 213.
[7] M. Stavrev, D. Fischer, C. Wenzel, K. Drescher, N. Mattern, Thin Solid Films 307 (1997) 79.
[8] M. Sikkens, I.J. Hodgkinson, F. Horowitz, H.A. Ma closed, J. Wharton, Opt.Eng. 25 (1986) 142.
[9] A.L. Barabasi, H.E. Stanley, Fractal Concepts in Surface Growth, Cambridge University Press, New York, 1995.
[10] T. Vicsek, Fractal Growth Phenomena, World Scientific, Singapore, 1989.
[11] B.B. Mandelbrot, The Fractal Geometry of Nature, Freeman, NewYork, 1982.
[12] J. Krim, I. Heyvaert, C. Van Haesendonck, Y. Bruynseraede, Phys. Rev. Lett. 70 (1993) 57.
[13] S. Hoseinzadeh, A.H. Ramezani, J. Nanostruct. 9 (2019) 276–286.
[14] A.H. Ramezani, S. Hoseinzadeh, A. Bahari, J. Inorg. Organomet. Polym. Mater. 28 (2018) 847–853.
[15] A.H. Ramezani, S. Hoseinzadeh, Zh. Ebrahiminejad, Mod. Phys. Lett. B (2020).
[16] T. Gredig, E.A. Silverstein, M.P. Byrne, J. Phys. Conf. Ser. 417 (2013) 012069.
[17] V.N. Bliznyuk, V.M. Burlakov, H.E. Assender Briggs, G.A.D. Tsukahara, Macromol. Symp. 167 (2001) 89.
[18] A. Le Gal, L. Guy, G. Orange, Y. Bomal, M. Kluppel, Wear 264 (2008) 606.
[19] D. Raoufi, F. Hosseinpanahi, Appl. Phys. 7 (2013) 21.
[20] K. Ghosh, R.K. Pandey, Appl. Phys. A 125 (2019) 98.
[21] K. Ghosh, R.K. Pandey, AIP Conf. Proc. 2115 (2019) 030280.
[22] K. Ghosh, R.K. Pandey, Mater. Res. Express 6 (2019), 086454.
[23] J.A. Ogilvy, J.R. Foster, J. Phys. D Appl. Phys. 22 (1989) 1243.
[24] I. Simonovski, L. Cizelj, International Conference. Nuclear Energy for New Europe, 110, 2005, p. 1.
[25] G. Palasantzas, J. Barnas, Phys. Rev. B 56 (1997) 7726.
[26] G. Palasantzas, J. Barnasa, Th.M. De Hosson, J. Appl. Phys. 88 (2000) 927.
[27] Y. Zhao, G.-Ch. Wang, T.-M. Lu, Characterization of Amorphous and Crystalline Rough Surface: Principles and Applications, Department of Physics, Applied Physics, and Astronomy Rensselaer Polytechnic Institute Troy, New York, 2001.
[28] D. Raoufi, F. Hosseinpanahi, J. Theor. Appl. Phys. 7 (2013) 21.
[29] W.-Z. Wang, H. Chen, Y.-Z. Hu, Wang. Tribol. Int 39 (2006) 522.
[30] F.L. Forgerini, W. Figueiredo, Phys. Rev. E 79 (2009) 041602.
[31] F.D.A. Aarão Reis, Physica A 364 (2006) 190.
[32] F.A. Silveira, F.D.A. Aarão Reis, Phys. Rev. E 75 (2007) 061608.
[33] A.H. Ramezani, M.R. HantehzAdeh, M. Ghorannevis, E. Darabi, Appl. Phys. A 39 (2016) 122.
[34] L. Sun, Zh. Shi, H. Wang, K. Zhang, D. Dastan, K. Sun, R. Fan, J. Mater. Chem. A 8 (2020) 5750–5757.
[35] L. Sun, Z. Shi, L. Liang, S. Wei, H. Wang, D. Dastan, K. Sun, R. Fan, J. Mater. Chem. C 8 (2020) 10257–10265.
[36] Yin X-Tao, J. Li, D. Dastan, Zhou W-Dong, H. Garmestani, F.M. Alamgir, Chem 319 (2020) 128330.